Advances in Science and Technology Research Journal

Advances in Science and Technology Research Journal, 2026, 20(3), 226–239
https://doi.org/10.12913/22998624/214171
ISSN 2299-8624, License CC-BY 4.0

Received: 2025.09.13
Accepted: 2025.11.12
Published: 2026.02.01

Sustainable superhydrophobic composite nanofiber membranes for desalination via air gap membrane distillation

Safa N. Mohammed[1], Basma I. Waisi[1*]

[1] Department of Chemical Engineering, College of Engineering, University of Baghdad, Baghdad, Iraq
* Corresponding author's e-mail: basmawaisi@coeng.uobaghdad.edu.iq

ABSTRACT

Super-hydrophobic nanofiber membranes have recently demonstrated significant potential as desirable approaches for membrane distillation and are favored because of their high vapor flux and remarkable salt rejection capabilities. This paper presents the design and testing of electrospun nanofiber membranes developed from recycled acrylic combined with different silica nanoparticle concentrations, namely (0, 1, 2, and 3 wt.%), to be used in high-salinity brine desalination using air gap membrane distillation. The use of recycled acrylic provides a sustainable, eco-friendly, and low-cost alternative to conventional petroleum-based polymers. The incorporation of silica nanoparticles led to a decline in both fiber diameter and pore size, as well as an increase in surface hydrophobicity. For the composite RA/3 wt.% silica membrane, the water contact angle reached 138 ± 2°. Fourier-transform infrared spectroscopy was used to evaluate the RP and verify the incorporation of silica. The membrane's peak performance in the MD system was observed across a range of feed temperatures (45–65 °C), flow rates of 0.2 to 0.4 L/min, and NaCl concentrations (35–140 g/L). Its higher temperatures and flow rates corresponded to higher permeate flux. However, as the concentration of salt increased, the vapor pressure decreased, the concentration polarization became more serious, and the permeate flux decreased. Best performance was at 65 °C and 0.3 L/min, in which the maximum flux of 9.5 kg/m²h and salt rejection > 99.999% were obtained. These results indicate that the RA-based superhydrophobic silica composite membranes could be a potential green and low-cost candidate for sustainable desalination in the AGMD process.

Keywords: desalination, air gap membrane distillation (AGMD), hydrophobic polymer, nonwoven nanofibers, silica nanoparticles.

INTRODUCTION

The significance and worth of water have become increasingly emphasized in recent times, attributed to the surging global population, swift industrial growth, andurban development [1]. Reports indicate that the global population has tripled, while water consumption has surged more than six times throughout the 20th century, highlighting an increase in the number of water consumers. Under such conditions, it is understood that exploration in several saline water sources, including the oceans and brackish sources, as well as methods for turning saltwater into freshwater, have become viable in recent generations as a strategy to alleviate freshwater scarcity and support the universal need for water. [2]. As such, figuring out how to addressing issues in a cost-effective and energy-efficient manner has emerged as a crucial approach to tackling the challenge of water scarcity [3]. Considering these membrane distillation technologies (MD), which are emerging as a promising alternative method for water desalination, provide even higher water quality [4]. This process utilizes a thermally driven membrane separation mechanism that capitalizes on the transmembrane vapor pressure difference, which is produced by temperature difference across the membrane serves as the motivating factor for the generation and movement of product vapor [5]. The MD have many advantages, including (a) its tolerance to

high salinity brines, (b) high salt rejection (c) low fouling and low operating pressure (near atmosphere), (d) lower sensitivity to concentration polarization and fouling with respect to other membrane separation processes like RO, and (e) high compactness and low weight. The primary disadvantage of these methods is the comparatively low rate of permeate flow, along with the moisture retention within the membrane's pores. This issue is influenced by fouling or scaling, which in turn impacts both the quality of the water and the overall productivity [6–9].

There are many different configurations membrane distillation (MD) modules can be categorized based on their vapor condensation methods. These include:

a) Direct contact membrane distillation (DCMD), where the cooling solution directly interacts with the membrane on the permeate side
b) Air gap membrane distillation (AGMD), which features an air gap between the membrane and the condensation surface to minimize heat loss through conduction, with vapor condensing on a cold plate located within the permeate;
c) Sweeping gas membrane distillation (SGMD), where an inert gas is circulated through the permeate to transport the water vapor, which is subsequently condensed outside the membrane module; d) vacuum membrane distillation (VMD), in which a vacuum is applied to the permeate side of the membrane module, facilitating the escape of vapor outside the module for condensation [9,10].

MD employs specially designed microporous membranes that prevent wetting, serving as a liquid/vapor interface for the diffusion of water vapor. The hydrophobic nature of these membranes holds back the liquid feed solution, while their microporous architecture permits the passage of vapor. For optimal mass transfer and energy efficiency, MD membranes should ideally possess a balanced pore size, substantial porosity, and a hydrophobic exterior. Furthermore, it is crucial to control the membrane's thickness to enhance both vapor permeability and overall energy efficiency [11]. If the hydrophobic characteristics are insufficient, the membrane may become saturated with the feed solution, leading to unstable operation [12–14].

Compared to other methods of MD membrane preparation, electrospun nanofiber membranes (ENMs**)** have attracted growing interest in the MD process because their characteristics comprise a high surface area-to-volume ratio, adaptable surface functionalities, naturally high porosity, fully interconnected pore structures, low hydraulic resistance, and the ability to be produced on a large scale [15,16]. The electrospinning techniques ultimately simplify fiber formation, which is fabricated via a process where a high-voltage power supply energizes a stream of fluid that passes through a capillary tube, producing thin fibers from polymer melts or solutions [17]. Various types of polymers were used to produce nonwoven nanofiber membranes, such as polypropylene (PP) [18], polyvinylidene fluoride (PVDF) [19], and polytetrafluoroethylene (PTFE) [20]. Inevitably, though, such fossil-source polymeric membranes increase their demand year by year to a point which becomes too much to bear to a range of factors, such as the deposition of unanticipated fouling and mechanically/chemically induced defects [21,22]. Moreover, the use of these monomer/polymer compounds in everyday items has created a new problem in the disposal of post-utilization waste [23,24].

Therefore, the development of waste material recycling potential for use in membrane fabrication will reduce pollution by a certain amount, thus assisting with the maintenance of environmental sustainability. The material not only reduces the plastic waste and environmental pollution, but it also offers a cheap substitute for virgin polymers, thereby pushing up membrane product output, for example, of proportionally generated waste polystyrene [25], polyethylene terephthalate[26], tire rubber, and keratin [27].

Various methods are being utilized to enhance the efficiency of MD membranes, such as coating with hydrophobic nanoparticles [28], using surface modifying macromolecules (SMMs) [29], blending [30], incorporating nanofillers [31], and employing multi-layered [32], hydrophobic/hydrophilic designs [33]. However, assessing the costs and possible environmental hazards associated with these substances has underscored the significance of exploring and creating alternative materials. Engineered nanomaterials (ENMs) can be developed using nanoparticles (NPs) to form hierarchical surface structures. This process enhances surface roughness and generates multiple air pockets, resulting in improved hydrophobic properties and wetting resistance with nanomaterials for MD application due to their low surface energy,

non-toxicity, and low cost [34], improves flux and fouling [35], and produces an anti-surfactant-wetting [36].

Although silica dioxide SiO_2 nanoparticles were used to successfully incorporate into the membrane framework [37]. However, the addition of silica nanoparticles to electrospun membranes is primarily restricted to physical blending because silica does not dissolve in solvents. This method often leads to inevitable particle aggregation when high quantities are used, along with poor compatibility between the silica and the polymer blend. Therefore, achieving a uniform distribution of silica on the membrane surface requires a strong interaction between the fillers and the polymers[38]. Superhydrophobic electrospun nanofiber membranes (ENMs) were prepared from polyvinylidene fluoride (PVDF) solutions containing silica nanoparticles (0–6 wt.%) for the formation of multiscale surface roughness. After acid pretreatment and modification with fluoroalkylsilane (FAS), the developed composite membranes (FAS–Si@PVDF-A) at 6 wt.% SiO_2 showed higher wetting resistance – a water contact angle (WCA) of 154.6 ± 2.2°, smaller average pore size of 0.27 ± 0.03 μm, and larger liquid entry pressure (LEP) of 143 ± 4 kPa. In vacuum membrane distillation (VMD) tests using 3.5 wt.% NaCl feed solution, the optimized membranes (thickness 98 ± 5 μm) achieved a stable permeate flux of >11.5 $kg \cdot m^{-2} \cdot h^{-1}$ and salt rejection of 99.9% over 22 h of continuous operation [39].

This research fills a need for cost-effective, high-quality materials in water treatment and circles back to utilizing post-consumer acrylic waste for membrane manufacture, helping to complete the circular economy. Due to its insolubility and mechanical robustness, it shows great potential for a membrane application. Furthermore, the use of recycled acrylic material is much cheaper than obtaining new polymer. In view of this perspective, the research aims at preparing nanofiber polymeric nonwoven membranes by electrospinning. In this paper, we have successfully fabricated water desalination membranes by air gap membrane distillation (AGMD) using hydrophobic recycled acrylic (RA) membrane-based nanofibrous materials at different silica nanoparticle loadings (0, 1, 2, and 3 wt.%). The RA-based membranes were characterized using scanning electron microscopy (SEM), assessment of mechanical characteristics, determination of WCA, and Fourier transform infrared spectroscopy (FTIR). After identifying the optimal membrane, an extensive analysis was performed to assess how different operational parameters – like feed temperature, flow rate, and salt concentration – affected the distillation efficiency in the AGMD system.

MATERIALS AND METHODS

Materials

It was used in work with waste acrylic hard plastic; specifically, polymethyl methacrylate (PMMA), marketed under various trade names, including Perspex, was sourced from an advertising shop and is primarily used to prepare a recycled acrylic (RA) powder. The silica dioxide (SiO_2) (density: 2.4 g/cm^3) standard particles measuring between 10 nm and 1.5 μm are non-porous particles. It was supplied by Alfa Aesar with a purity of 99.99%. The organic solvents N, N-dimethylformamide (DMF) with a density of 0.948 g/cm^3 and chloroform ($CHCl_3$) which has a density of 1.49 g/cm^3 were provided by Alfa Aesar and employed to dissolve the recycled RA. Sodium chloride (NaCl), obtained from Sigma-Aldrich, was employed to create the saline (brine) feed solutions for the membrane distillation experiments. All chemical materials were used in their form without any additional modifications

Nonwoven nanofiber membranes via electrospinning system

In this study, the recycled acrylic (RA-based) nanofiber membranes were fabricated using the electrospinning approach with additional silica dioxide as an improvement and reinforcing material. A mixture was prepared containing 15% of RA and (0,1, 2, and 3 wt.%) SiO_2 nanoparticles. Firstly, a solvent mixture of $CHCl_3$/DMF (15:70)% was prepared by stirring at 150–250 rpm for a duration of 15 minutes. Subsequently, pieces of hard acrylic plastic waste were ground into smaller fragments with an electric grinder, added to the $CHCl_3$/DMF solvent, and the mixture was stirred for 5 hours at room temperature until a clear and homogeneous spinning dope was obtained [40].

The electrospinning apparatus was made up of a syringe pump, a high-voltage power source, and a rotating drum; more details are in our

previous work [41]. The homogeneous precursor solutions were transferred into a 5 mL plastic syringe equipped with a narrow inner diameter and a capillary metal gauge needle (21 × 11/2”). The polymeric solution was dispensed at a rate of 2 mL/h, with the distance from the tip to the collector set at 13 cm. The electrospinning was performed at room temperature, while the spinning apparatus maintained an ambient humidity level of 20%. Each membrane exhibited uniform thickness and was produced under consistent process parameters. A high-voltage electrostatic field ranging from 18 to 25 kV was employed to create all nanofiber membranes throughout the electrospinning procedure. The polymer jets were released and collected on a rotating drum, through the vaporization of the solvent, leading to the formation of a mat of nonwoven nanofibers on the collector’s surface [42], with dimensions of approximately 13 × 30 cm. After electrospinning, the dried membranes were then stored in clean plastic containers to prevent contamination before characterization and testing [43].

Membrane characterization

Membrane microstructure

A scanning electron microscope (SEM) is an advanced tool that focuses a high-energy electron beam onto a sample’s surface for sample analysis. The microscope collects the signals that the specimen emits through some detectors. The images depicting the membrane structure were obtained using an analytical electron microscope (National Institutes of Health SEM, USA). The obtained images subsequently facilitated evaluation of the prepared nanofiber nonwoven membrane’s surface topography and morphology from RA.

Surface hydrophobicity

The hydrophobic properties of the membrane can be assessed by evaluating the contact angle (Theta Lite TL101, Biolin Scientific, USA) of the membranes. A drop of distilled water was carefully placed on the membrane surface. After the droplet finally stabilized, an image was recorded with a built-in camera before the software automatically calculated its contact angle. The larger the contact angle means the greater hydrophobicity of the membrane: the smaller area touches against water, and so it has greater resistance to wetting.

Fourier-transform infrared spectroscopy (FTIR)

It is utilizing the Spectrum 1800 model from Shimadzu, Japan, and serves as an effective analytical method in the field of chemistry. This technique is utilized to identify different types of molecules, including their functional groups, by directing radiation through a sample. As the radiation interacts with the sample, part of the infrared radiation is absorbed, while the remainder is transmitted. The spectrum obtained reflects the absorption and transmission characteristics of the molecules present [44,45] developing a molecular signature of the sample, and operating in the 4000–400 cm^{-1} or 4000–600 cm^{-1} wavenumber range.

Mechanical properties

A crucial factor to consider for any practical application is the mechanical properties of membranes, which encompass their reusability, ease of handling, and resistance to deformation [46]. The mechanical properties of the membranes were tested by examining the breaking strength and Young’s modulus of the membrane specimens, determined by a dynamic mechanical analyzer (DMA) (AG-A10T, Shimadzu, Japan). The rectangular samples measured 10 cm in length and 1 cm in width, with assessments conducted at a temperature of 25 °C and under standard humidity conditions. Young’s modulus serves as an indicator of tensile strength by illustrating the ratio between stress and strain. However, it is important to note that flexible materials generally demonstrate a lower Young’s modulus[47,48].

Air gap membrane distillation (AGMD) system

The permeability flux through the membrane is calculated using the following equations [49]:

$$J = \frac{V \times \rho}{A \times t} \quad (1)$$

where: the permeate flux is represented in J (kg/m².h), V is the freshwater volume (L), ρ is the water density (kg/L), t is the operational time (hours), and A is the effective surface area of the membrane in m².

The Salt rejection (R%) is estimated using the following equation:

$$R\% = 1 - \frac{C2}{C1} \times 100 \quad (2)$$

where: R is the salt retention, $C1$ is the feed concentration, and $C2$ is the concentration of the permeate. The used membrane distillation system consisted of three compartments, as displayed in more detail in our previous work [17]. Heating of the feed solution is accomplished by the heater (bath water), and a pump recirculates water in the upper part, and a control valve and a pressure gauge on the right side control the flow rate.

Moreover, coolant circulates through the bottom (chiller), while a pressure gauge and control valve are positioned on the left side for monitoring purposes, the collected permeate is contained within the central chamber and organized in a measuring cylinder. In the membrane module, the feed and coolant circulate in opposing directions within a closed-loop system. The membrane is situated between the feed compartment and an air gap, with the vaporized water flowing downward through a stagnant air gap that lies between the membrane and a condenser plate [50]. The temperatures of the feed water and coolant at both the inlet and outlet were consistently monitored using industrial-grade temperature sensors. Four sensors were utilized in total; two were installed at different points on the feed side, while the remaining two were located on the coolant side.

In the AGMD configuration, a membrane module was developed, incorporating a 6 mm air gap. The chamber dimensions in this setup are 1.5 cm in thickness, 7 cm in length, and 7 cm in width. A water bath was utilized to heat the prepared brine water to various temperatures ranging from 45 to 65 °C, after which it was cooled to a stable temperature of 15 °C. Different concentrations of brine solution were created by weighing out 35, 70, and 140 grams with a precise balance (Kern-PLE 310-3N), and each measured amount was dissolved in one liter of distilled water containing sodium chloride, serving as the feed solution. AGMD experiments were conducted for 180 minutes for each set of experimental conditions. The concentration of salts in both the feed and permeate entering and exiting the membrane module was accurately measured using a commercial digital meter (Handheld TDS EC pH temp Salinity meter). The system's performance was assessed based on the permeate flux (kg/m²·h) and salt rejection [51].

RESULTS AND DISCUSSION

Membrane characterizations

Electrospinning serves as a widely used and established method for producing MD membranes characterized by high porosity, superior hydrophobic properties, and an adjustable nonwoven porous structure that offers substantial surface area and functionality. This research involved the creation of nanofibrous membranes through electrospinning, utilizing solutions containing different concentrations of SiO_2 nanoparticles. These SEM images of membrane cross-sections were taken using ImageJ. Every kind of sample represented in Figure 1 had long, straight fibers with smooth surfaces and uniform diameters. No evidence was found for there being a bead or surface defect; these results ensure that the electrospinning process was stable and that fibers were formed homogeneously. In ImageJ, we found that the pure RA-based membranes had a mean diameter of 12.9 µm. With the addition of 1 wt. % SiO_2 nanoparticles, this fell to 12.1 µm. At concentrations of 2 and 3 wt.%, the diameters of the fibers were further reduced to 11.7 and 11.5 µm, respectively. The cause of this decline is that when the spinning solution's electrical conductivity

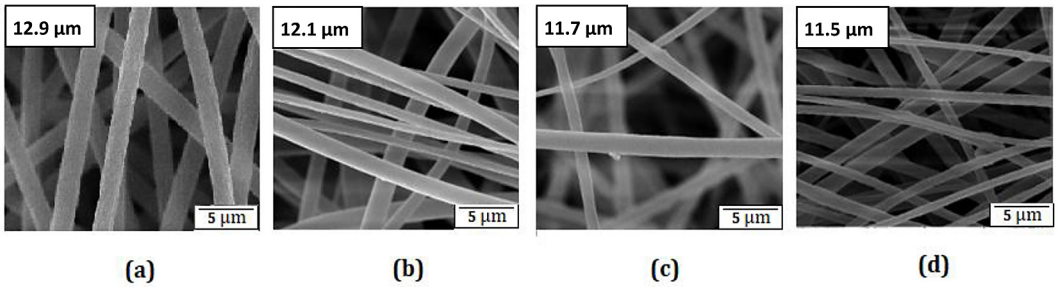

Figure 1. The surface morphology of the prepared recycled acrylic-based non-woven nanofiber membranes with embedded SiO_2 in varying amounts (a) 0%, (b)1%, (c) 2%, and (d) 3 wt.%

is enhanced, the thermal and electric resistance encountered by stretching fibers is inevitably decreased. This phenomenon can be reasonably referred to as "redoubling or halving-cost benefit effect, due to the greater numbers produced when an order is placed with a diminishing unit piece price. Here, it means that higher incorporation of SiO_2 brings greater change in solution viscosity and subsequently to thinner fibers [52].

At higher nanoparticle loadings, silica tended to aggregate on the fiber surface as a result of its diminutive size and elevated surface energy. These agglomerations, although sometimes enhancing surface roughness and hydrophobicity, generally decrease membrane uniformity, porosity, and mechanical strength. Nevertheless, the random orientation of fibers produced a highly porous structure, which is advantageous in MD applications because it facilitates vapor transport, minimizes thermal conductivity, and reduces the risk of pore wetting, ultimately improving mass transfer performance.

The composition of the chemicals in the membranes that were developed from RA-based non-woven nanofiber membrane by Fourier Transform Infrared Spectroscopy FTIR (Figure 2a). The peaks observed at 3022.45–3057.17 cm^{-1} are attributed to alkenic C–H stretching vibrations [53]. While the strong absorptions in the 2920.23–2846.93 cm^{-1} range correspond to C–H stretching of $–CH_3$ and $–CH_2–$ groups, consistent with the aliphatic backbone of RA-baes. It is also observed that the peak at 1749.5 cm^{-1}, along with the broader range from 1743.65 to 1940.39 cm^{-1}, represents the C=O stretching vibration of ester groups, confirming the presence of acrylic components in the nanofiber membrane [54]. The bending vibrations of CH_2 and CH_3 groups are evident at 1490.97 and 1371.39 cm^{-1}, respectively. In the 1200–1000 cm^{-1} region, multiple peaks correspond to C–O–C stretching vibrations of the ester moiety. Furthermore, peaks in the 840–600 cm^{-1} region (including 754.17 and 698.23 cm^{-1}) are linked to bending that occurs out of the plane of $–CH_2$ groups or side-chain vibrations. It is also posited that the peak at 1668.43–1600.92 cm^{-1} represents the C=O stretching vibration of ester groups, verifying the presence of acrylic components in the nanofiber membrane [54]. All these spectral bands, combined together, reveal the satisfactory synthesis of RA-based nanofibers retaining their ester groups, and the high chemical purity of the electrospun membrane was confirmed, as no intensive bands belonging to either degradation or contamination were observed.

The analysis of the spectrum of the embedded SiO_2 in the RA membrane exhibits intensity bands at 1157.29–1028.06 cm^{-1}, bands indicate the existence of silica nanoparticles distributed throughout the membrane matrix. This implies that silica is present in small amounts and serves as a surface or nanoscale additive intended to improve specific properties that correspond with [55,56]. Furthermore, relate the very strong rise at 906.54–698.23 cm^{-1} to the out-of-plane bends of Si-O groups is easily explainable as a Si-O stretching that also became sharper and more intense, confirming the successful incorporation of SiO_2 nanoparticles as the concentration increased. Such spectral features are able to confirm that RA-based has been successfully made into nanofibers containing integrated SiO_2 functions and that no substantial contamination or deterioration occurred during the process.

The WCA (Water Contact Angle) assessed for all altered membranes varied from 122 ± 2 to 138 ± 2, indicating hydrophobicity This phenomenon was noted in all membranes fabricated with nanofibers, and this achievement was documented, as illustrated in Figure 3, the contact angle for different nanofiber membranes escalates rapidly as the concentration of silica nanoparticles increases from 0 wt.% to 3 wt.%. A comparison of the WCA of the unmodified RA membrane before and after the modification reveals a significantly hydrophobic surface, exhibiting strong water-repellent capabilities that hinder water from wetting the surface. The optimal performance of the modified membrane at RA with 3 wt.% SiO_2 resulted in a considerably enhanced contact angle of 138 ± 2°. The improved performance of the changed membrane can be seen from the silica nanoparticles newly applied to the surface and the adhesive ability of hydrophobic silane groups, as a result of its increased surface roughness. It is different from the smooth nanofibers of RA membranes, which had not been modified in any way. The significant rise in water contact angle (WCA) was not noted in the pristine RA membrane, which absence nanoparticles.

Mechanical stability of the membranes was evaluated by measuring their breaking strength and Young's modulus. Figure 4, shows the curve of electrospun membranes produced from RA with SiO_2 nanoparticles. The mechanical properties of nanocomposites depend to a great extent

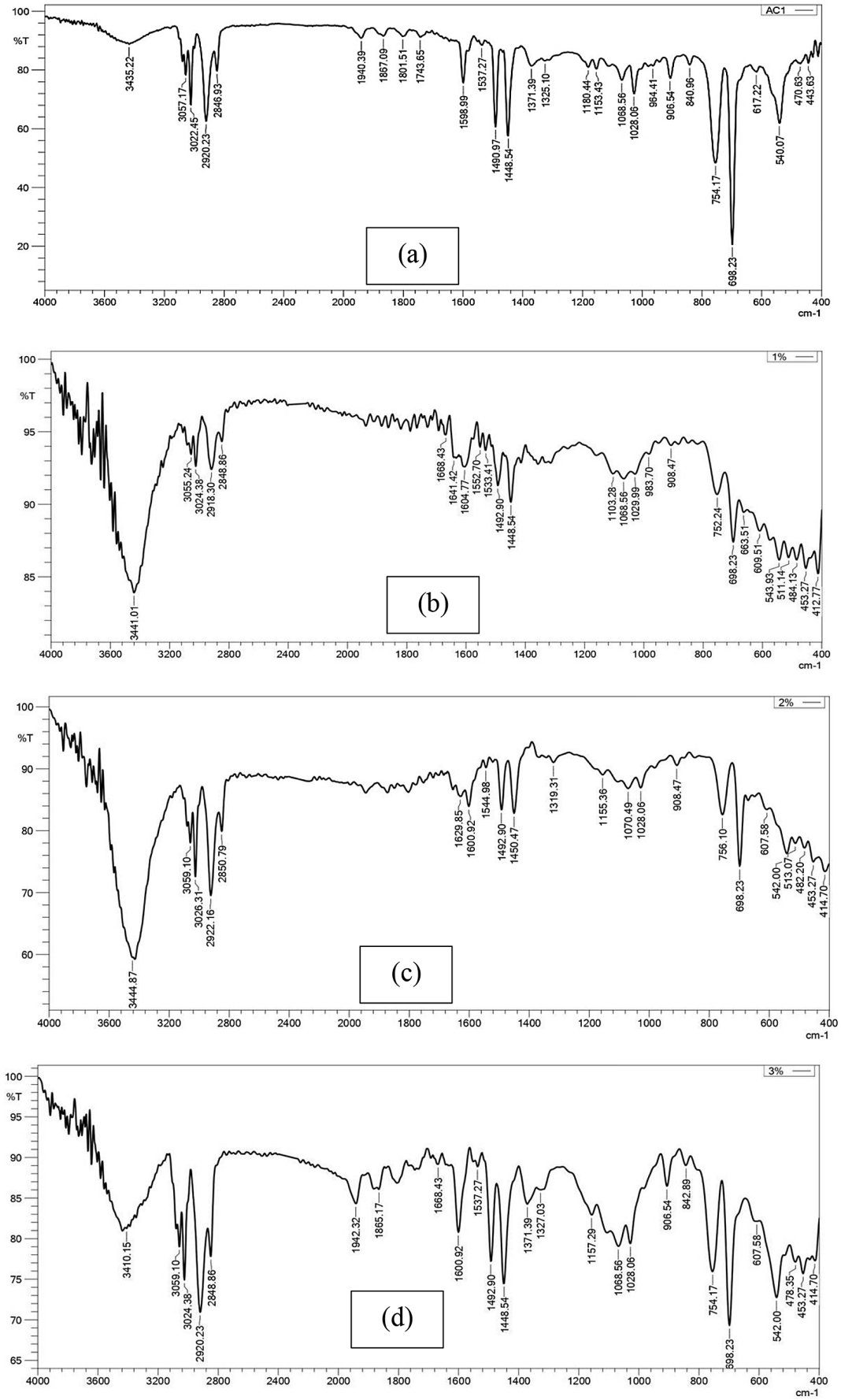

Figure 2. The FTIR spectra of RA-based nanofiber membranes containing varying levels of silica nanoparticles: (a) 0 wt.%, (b) 1 wt.%, (c) 2 wt.%, and (d) 3 wt.%

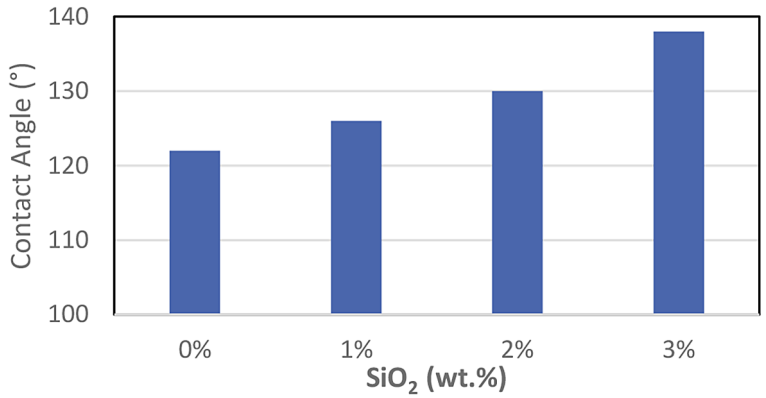

Figure 3. Water contact angles of RA-based nanofibrous membranes with varying quantities of silica nanoparticles from 0 to 3 wt.% SiO_2

on the distribution of nanoparticles in the polymer solution. Nevertheless, if the surface of the nanoparticles is appropriately modified and good processing conditions are available, it is feasible to ensure an excellent dispersion of nanoparticles. As a follow-up, ripple tests were performed and the experimental data showed that the recycled acrylic (RA) sheets with uniformly dispersed silica nanoparticles had significantly better mechanical properties. In addition, the RA membrane infused with SiO_2 with a weight of 3 wt.% had greater stress capacity, comparable to other two kinds of membranes, as the fiber produced with the electrospinning process had stronger bonding forces between fibers. Increasing the concentration of SiO_2 nanoparticles results in strengthening the tensile strength of the electrospun nanofiber membrane. The increase of polymer concentration and the percentage of nanoparticles make the polymer chain contact and entangle, raising the number of polymer chains as the fiber is generated. Additionally, the larger the fiber is, the more residual solvent the fiber center encapsulates due to capillary squeeze. As a result, fiber bonding is further strengthened during solvent evacuation, resulting in a stronger electrospun nanofiber membrane.

Membrane performance test

In order to test how well the engineered membranes worked when desalting brine water, we conducted experiments with an air gap membrane distillation (AGMD) system. Critical operational factors such as feed temperature, feed flow rate, and salt concentration were investigated in this study. There was an exploration of permeate flux performance. The aim was to find out an optimal operational condition that is most beneficial for flux improvement. On the cold side, we held the temperature and flow rates fixed at 15 °C and 0.3 L/min respectively. However, different temperatures on the hot side inlet point were selected: 45 °C in one group, 55 °C in the second group, and 65 °C in the third group. In addition, the flow rate on both the hot and cold sides was adjusted to (0.2, 0.3, and 0.4) L/min. As for the feed solutions to test the membrane performance, the test solutions were prepared from NaCl brines with concentrations of (35, 70, and 140 g/L) to simulate industrial water and seawater (brine-rich amount of NaCl) at lab scale. It is essential to emphasize that the engineered membrane of RA-based material containing 3.0 wt.% SiO_2 was adopted after a series of trials presented in the current work.

The influence of feed temperature

The efficiency of MD systems is particularly affected by fluctuations in feed temperature, especially on the hot side of the module, making effective temperature regulation essential for maximizing water recovery efficiency. as illustrated in Figure 5. feed temperatures were set between 45 °C and 65 °C, with everything else kept constant, including a brine concentration of 35 g/L and a feed flow rate of 0.3 L/min. When the temperature rises, there should be expected to be a substantial exponential increase in the vapor pressure with respect to boiling point temperature. Furthermore, the increase in temperature makes it easier for vapor to move through the membrane.

It is shown in Antoine's equation that gas pressure is an exponential function as temperature increases. In the case of mass transfer of gas

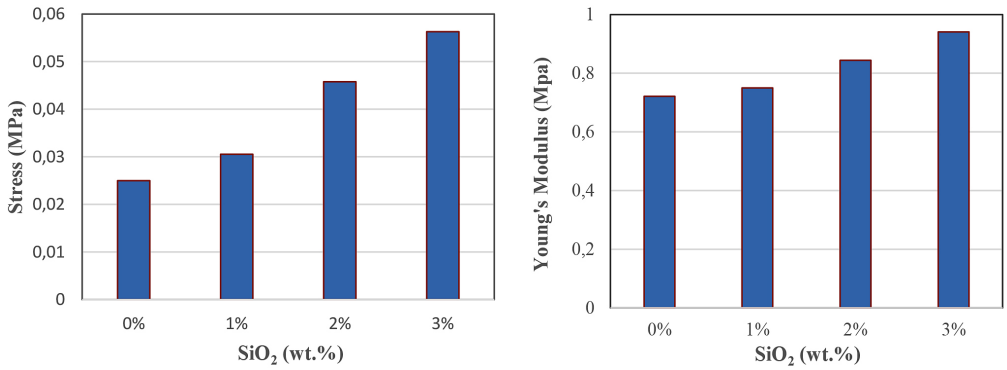

Figure 4. Membrane mechanical properties (strength and Young's modulus) of RA-based nanofiber membranes containing varying amounts of silica nanoparticles from 0 wt.% to 3 wt.%

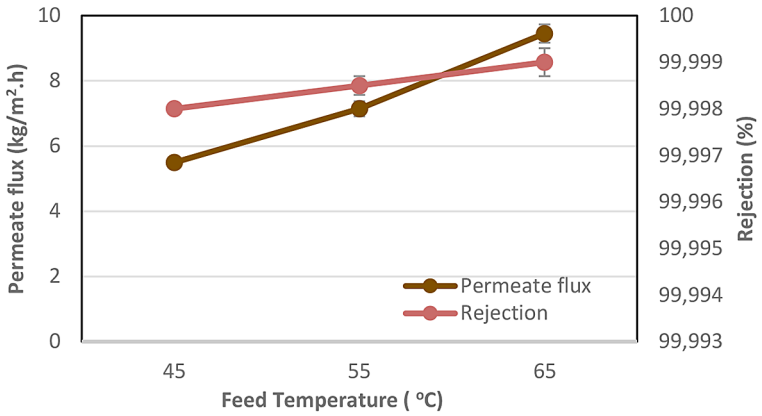

Figure 5. The influence of feed temperature (45–65 °C) on the permeate flux of RA-based containing wt.% SiO_2 membrane at 0.3 L/min and 35 g/L NaCl

through membranes, this function becomes the primary motivation for movement across a membrane distillation system [57]. The highest flux was also the one to 9.5 kg/m²h at 65 °C, adopting this temperature as the optimal condition to operate studied in this study not only confirmed its practicality but also took into account its practical applicability in real-world desalination systems. Good performance and high-water recovery were all things the temperature of 65 °C thereby supporting its suitability for efficient brine treatment AGMD technology, therefore, it is suitable for flexible salt farming. The membrane always had good desalting performance. Salt rejection values between 99.9989% and 99.999% were apt.

The influence of feed flow rate

The feed flow rate plays a decisive role in determining how much heat and mass transfer occurs in the membrane module, and this consequently affects the performance of membrane distillation (MD) systems. Tests were conducted at a temperature of 55 °C and a NaCl concentration of 35 g/L, with the feed flow rate adjusted between 0.2 and 0.4 L/min as to investigate how this would affect AGMD. As illustrated in Figure 6, the distillate flux exhibited an almost linear increase with the flow rate, enhancing AGMD efficiency, with the permeate flux achieving 8.05 kg/m²h. This improvement is linked to the heightened turbulence in the flow channel, which facilitates better mixing and mass transfer across the acrylic membrane containing 3 wt.% SiO.

The Reynolds number, of course, rises as the flow rate increases and, in turn, the hydrodynamic laminar layer gets thinner, which improves the heat transfer coefficient and thus reduces feed-side temperature polarization[58]. Significantly, even though flow rates were increased, all membranes in the present study exhibited excellent separation performance; salt rejection everywhere was 99–99.999%.

The influence of feed salt concentration

The feed salt concentration, e.g., a brine solution or seawater, has a significant effect on the

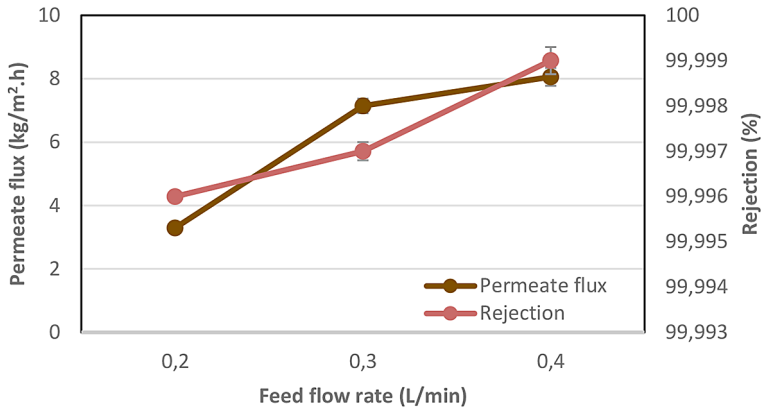

Figure 6. The influence of feed flow rate (0.2–0.4 L/min) on permeate flux of RA-based membrane containing 3 wt.% SiO_2 at 55 °C and 35 g/L NaCl solution

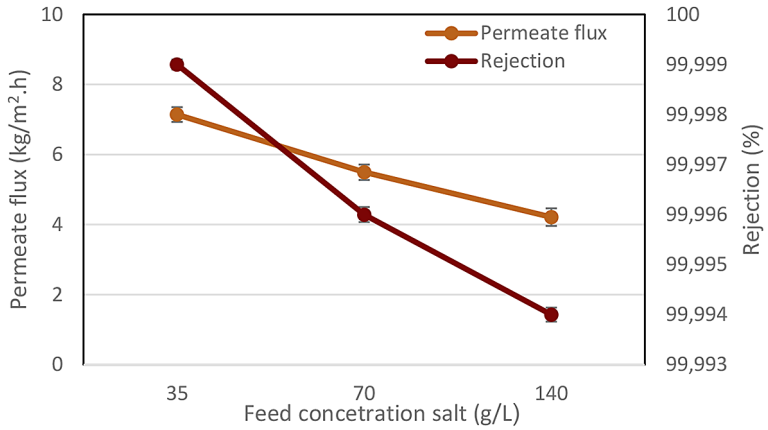

Figure 7. The influence of NaCl concentration (35–140 g/L) on the permeate flow of a recycled acrylic-based material membrane containing 3 wt.% SiO_2 on the surface at 55 °C and 0.3 L/min

performance of AGMD systems, as it does on all membrane separation technologies [59]. The effect of feed salinity was assessed by changing the salt concentration from 35 to 140 g/L, while all other parameters were kept the same (i.e., 0.3 L/min and 55 °C constant), As shown in Figure 7, the results reveal a significant reduction in the distillate flux as the salt concentration increases This reduction in efficiency may be due to a number of factors; first, with the increase of salt concentrations, the vapor pressure of the feed solution decreases, and the mass transfer driving force is reduced. Additionally, there may be an increase in concentration polarization occurring at the membrane surface, which can reduce membrane efficiency over time [60]. the constructed hydrophobic membranes maintained excellent salt rejection capabilities, with values ranging from 99.999% to 99.994%, indicating their strong potential for high-salinity desalination applications.

CONCLUSIONS

This study used electrospinning to successfully create superhydrophobic layers using RA as a sustainable polymer source for nanofiber membranes, adding nanoparticles of SiO_2 that are very organically wetted. The characterization studies of the produced membranes showed that the spinning nanofiber RA-based membrane containing 3 wt.% SiO_2 maintained its excellent morphological and physicochemical properties, including a highly porous and uniform fiber network and strong hydrophobicity (contact angle >138°). The electrospun nanofiber membranes have the optimal characteristics for fibers, including their shape and mechanical properties, are long, continuous, and beadles' nanofibers. The findings reveal that an increase in silica concentration within the dope solution leads to a corresponding rise in the water contact angle of the membrane. Additionally, this

rise in water contact angle is associated with a reduction in both the diameter of the nanofibers and the average pore size, while the functional groups containing the (SiO_2) group remain well-preserved. This is proven by FTIR results, which indicate no change in molecular state or storage temperature stability. The membranes underwent evaluation in a custom-built AGMD setup under various operating conditions, including feed temperatures ranging from 45 to 65 °C, flow rates between 0.2 and 0.4 L/min, and salt concentrations varying from 35 to 140 g/L. It was found that the feed water temperature had a more significant effect on permeate flux than the speed at which it flowed and the amount of salt in the solution, due to both increased vapor pressures (lowering temperature polarizations) and lower temperatures on the other side of the membrane. On the other hand, if feed water concentration increased, it had an adverse effect on flux through the membrane caused by increased mass transfer resistance and concentration polarization. At 65 °C and a flow rate of 0.3 L/min, with nearly 99.999% salt retention, the maximum observed reverse osmosis production rate approached 9.5 kg/m²·h, reflecting acclaimed features of these membranes as far as its selectivity and permanence. This study has demonstrated the technological and economic benefits of using waste-developed acrylic materials to make new types of high-performance water desalination membranes when compared with using full virgin polymers. By converting spent consumer acrylics into functioning membrane materials, the program embodies the Circular Economy philosophy and slashes plastic waste as well as being a scalable and environmentally friendly solution for producing clean water with membrane distillation technology.

REFERENCES

1. Gude V. G., Nirmalakhandan N., and Deng S., Low temperature process to recover impaired waters," Desalination Water Treat, 2010; 20(1–3), 281–290, https://doi.org/10.5004/dwt.2010.1613
2. Gude V. G., Energy storage for desalination processes powered by renewable energy and waste heat sources, Appl Energy, Jan. 2015; 137, 877–898. https://doi.org/10.1016/j.apenergy.2014.06.061
3. Feria-Díaz J. J., López-Méndez M. C., Rodríguez-Miranda J. P., Sandoval-Herazo L. C., and Correa-Mahecha F., Commercial thermal technologies for desalination of water from renewable energies: A state of the art review, Feb. 01, 2021, MDPI AG. https://doi.org/10.3390/pr9020262
4. Drioli E., Ali A., and Macedonio F., Membrane distillation: Recent developments and perspectives, Jan. 05, 2015, Elsevier. https://doi.org/10.1016/j.desal.2014.10.028
5. Khan A. M., Russo F., Macedonio F., Criscuoli A., Curcio E., and Figoli A., The state of the art on PVDF membrane preparation for membrane distillation and membrane crystallization: Towards the use of non-toxic solvents, Apr. 01, 2025, Multidisciplinary Digital Publishing Institute (MDPI). https://doi.org/10.3390/membranes15040117
6. Elmarghany M. R., El-Shazly A. H., Salem M. S., Sabry M. N., and Nady N., Thermal analysis evaluation of direct contact membrane distillation system, Case Studies in Thermal Engineering, Mar. 2019; 13, https://doi.org/10.1016/j.csite.2018.100377
7. Safi, Nawras N., and Basma I. Waisi, Enhanced hydrophobic double-layer nanofibers membranes for direct contact membrane distillation, Ecological Engineering and Environmental Technology, 2024; 25(4), 325–335, https://doi.org/10.12912/27197050/184224
8. S. M. Alkarbouly and B. I. Waisi, Fabrication of electrospun nanofibers membrane for emulsified oil removal from oily wastewater, Baghdad Science Journal, 2022; 19(6), 1238–1248, https://doi.org/10.21123/bsj.2022.6421
9. Luo A. and Lior N., Critical review of membrane distillation performance criteria," Desalination Water Treat, Sep. 2016; 57(43), 20093–20140, https://doi.org/10.1080/19443994.2016.1152637
10. Mejia Mendez D. L., Castel C., Lemaitre C., and Favre E., Membrane distillation (MD) processes for water desalination applications. Can dense selfstanding membranes compete with microporous hydrophobic materials?, Chem Eng Sci, Oct. 2018; 188, 84–96, https://doi.org/10.1016/j.ces.2018.05.025
11. Lee E.-J., An A. K., He T., Woo Y. C., and Shon H. K., Electrospun nanofiber membranes incorporating fluorosilane-coated TiO_2 nanocomposite for direct contact membrane distillation, J Memb Sci, Dec. 2016; 520, 145–154, https://doi.org/10.1016/j.memsci.2016.07.019
12. Xu J., Singh Y. B., Amy G. L., and Ghaffour N., Effect of operating parameters and membrane characteristics on air gap membrane distillation performance for the treatment of highly saline water, J Memb Sci, Aug. 2016; 512, 73–82, https://doi.org/10.1016/j.memsci.2016.04.010
13. Tomaszewska M., Membrane Distillation-Examples of Applications in Technology and Environmental Protection, 2000.

14. Yan K.-K., Jiao L., Lin S., Ji X., Lu Y., and Zhang L., Superhydrophobic electrospun nanofiber membrane coated by carbon nanotubes network for membrane distillation, Desalination, Jul. 2018; 437, 26–33, https://doi.org/10.1016/j.desal.2018.02.020
15. Al-Okaidy, Haneen S., and Basma I. Waisi., The effect of electrospinning parameters on morphological and mechanical properties of PAN-based nanofibers membrane, Baghdad Science Journal, 2023; 20,(4), 1433–1441, https://doi.org/10.21123/bsj.2023.7309
16. Tabe and Shahram, A review of electrospun nanofiber membranes article info, Journal of Membrane Science and Research, 2017; 3, 228–239, https://doi.org/10.22079/jmsr.2017.56718.1124
17. Safi N. N. and Waisi B. I., Preparation of electrospun double-layer PVDF: PMMA membrane non-woven nanofibers for desalination by membrane distillation process, Desalination Water Treat, Dec. 2023; 314, 49–58, https://doi.org/10.5004/dwt.2023.30063
18. Fang J., Zhang L., Sutton D., Wang X., and Lin T., Needleless melt-electrospinning of polypropylene nanofibres, J Nanomater, 2012; 2012, 1–9, https://doi.org/10.1155/2012/382639
19. Albiladi A., Gzara L., Organji H., Alkayal N. S., and Figoli A., Electrospun poly (vinylidene fluoride-co-hexafluoropropylene) nanofiber membranes for brine treatment via membrane distillation, Polymers (Basel), Jun. 2023; 15(12), https://doi.org/10.3390/polym15122706
20. Defor, Charles, and Shih-Feng Chou, Electrospun polytetrafluoroethylene (PTFE) fibers in membrane distillation applications, AIMS Mater Sci, 2024; 11(6), 1179–1198, https://doi.org/10.3934/MATERSCI.2024058
21. Khoo Y. S., Lau W. J., Hasan S. W., Salleh W. N. W., and Ismail A. F., New approach of recycling end-of-life reverse osmosis membranes via sonication for microfiltration process, J Environ Chem Eng, Dec. 2021; 9(6), 106731, https://doi.org/10.1016/j.jece.2021.106731
22. Landaburu-Aguirre J., García-Pacheco R., Molina S., Rodríguez-Sáez L., Rabadán J., and García-Calvo E., Fouling prevention, preparing for re-use and membrane recycling. Towards circular economy in RO desalination, Desalination, Sep. 2016; 393, 16–30, https://doi.org/10.1016/j.desal.2016.04.002
23. Tarek Ghaly S., Noby H., Hayashi J. i., and Elshazly A. H., Various waste polystyrene for useful membrane fabrication: Comparative experimental study, Mater Today Proc, Aug. 2023, https://doi.org/10.1016/j.matpr.2023.07.368
24. Zulfi A. et al., Air filtration media from electrospun waste high-impact polystyrene fiber membrane, Mater Res Express, Mar. 2018; 5(3), 035049, https://doi.org/10.1088/2053-1591/aab6ef
25. Aciu C., Manea D. L., Molnar L. M., and Jumate E., Recycling of polystyrene waste in the composition of ecological mortars, Procedia Technology, 2015; 19, 498–505, https://doi.org/10.1016/j.protcy.2015.02.071
26. Sharifian S. and Asasian-Kolur N., Polyethylene terephthalate (PET) waste to carbon materials: Theory, methods and applications, J Anal Appl Pyrolysis, May 2022; 163, 105496, https://doi.org/10.1016/j.jaap.2022.105496
27. Goh P. S., Othman M. H. D., and Matsuura T., Waste reutilization in polymeric membrane fabrication: A new direction in membranes for separation, Oct. 01, 2021, MDPI. https://doi.org/10.3390/membranes11100782
28. Ursino C., Di Nicolò E., Gabriele B., Criscuoli A., and Figoli A., Development of a novel perfluoropolyether (PFPE) hydrophobic/hydrophilic coated membranes for water treatment, J Memb Sci, Jul. 2019; 581, 58–71, https://doi.org/10.1016/j.memsci.2019.03.041
29. Khayet M., Suk D. E., Narbaitz R. M., Santerre J. P., and Matsuura T., Study on surface modification by surface-modifying macromolecules and its applications in membrane-separation processes, J Appl Polym Sci, Sep. 2003; 89(11), 2902–2916, https://doi.org/10.1002/app.12231
30. Prince J. A., Rana D., Singh G., Matsuura T., Jun Kai T., and Shanmugasundaram T. S., Effect of hydrophobic surface modifying macromolecules on differently produced PVDF membranes for direct contact membrane distillation, Chemical Engineering Journal, Apr. 2014; 242, 387–396, https://doi.org/10.1016/j.cej.2013.11.039
31. Ren L.-F., Xia F., Shao J., Zhang X., and Li J., Experimental investigation of the effect of electrospinning parameters on properties of superhydrophobic PDMS/PMMA membrane and its application in membrane distillation, Desalination, Feb. 2017; 404, https://doi.org/10.1016/j.desal.2016.11.023
32. Tijing L., Woo Y. C., Shim W.-G., Choi J.-S., Kim S.-H., and Shon H. K., Superhydrophobic nanofiber membrane containing carbon nanotubes for high-performance direct contact membrane distillation, J Memb Sci, Mar. 2016; 502, 158–170. https://doi.org/10.1016/j.memsci.2015.12.014
33. Khayet M., García-Payo M. C., García-Fernández L., and Martinez J., Dual-layered electrospun nanofibrous membranes for membrane distillation, Desalination, Jan. 2018; 426, 174–184, https://doi.org/10.1016/j.desal.2017.10.036
34. Afsari M., Li Q., Karbassiyazdi E., Shon H. K., Razmjou A., and Tijing L. D., Electrospun nanofiber composite membranes for geothermal brine treatment with lithium enrichment via membrane distillation, Chemosphere, Mar. 2023; 318, 137902, https://doi.org/10.1016/j.chemosphere.2023.137902

35. Kharraz J. A. and An A. K., Patterned superhydrophobic polyvinylidene fluoride (PVDF) membranes for membrane distillation: Enhanced flux with improved fouling and wetting resistance, J Memb Sci, Feb. 2020; 595, 117596, https://doi.org/10.1016/j.memsci.2019.117596
36. Huang Y.-X., Wang Z., Hou D., and Lin S., Coaxially Electrospun Super-amphiphobic Silica-based Membrane for Anti-surfactant-wetting Membrane Distillation, J Memb Sci, Feb. 2017; 531, https://doi.org/10.1016/j.memsci.2017.02.044
37. Wang S. et al., Preparation of a durable superhydrophobic membrane by electrospinning poly (vinylidene fluoride) (PVDF) mixed with epoxy-siloxane modified SiO_2 nanoparticles: A possible route to superhydrophobic surfaces with low water sliding angle and high water contact angle," J Colloid Interface Sci, Jul. 2011; 359(2), 380–388, https://doi.org/10.1016/j.jcis.2011.04.004
38. Jia W., Kharraz J. A., Choi P. J., Guo J., Deka B. J., and An A. K., Superhydrophobic membrane by hierarchically structured PDMS-POSS electrospray coating with cauliflower-shaped beads for enhanced MD performance, J Memb Sci, Mar. 2020; 597, 117638, https://doi.org/10.1016/j.memsci.2019.117638
39. Yadav P., Farnood R., and Kumar V., Superhydrophobic modification of electrospun nanofibrous Si@PVDF membranes for desalination application in vacuum membrane distillation, Chemosphere, Jan. 2022; 287, 132092, https://doi.org/10.1016/j.chemosphere.2021.132092
40. Subbiah T., Bhat G. S., Tock R. W., Parameswaran S., and Ramkumar S. S., Electrospinning of nanofibers, J Appl Polym Sci, Apr. 2005; 96(2), 557–569, https://doi.org/10.1002/app.21481
41. Al-Okaidy H. S. and Waisi B. I., The effect of electrospinning parameters on morphological and mechanical properties of PAN-based nanofibers membrane, Baghdad Science Journal, 2023; 20(4), 1433–1441, https://doi.org/10.21123/bsj.2023.7309
42. Diwan T., Abudi Z. N., Al-Furaiji M. H., and Nijmeijer A., A competitive study using electrospinning and phase inversion to prepare polymeric membranes for oil removal, Membranes (Basel), May 2023; 13(5), https://doi.org/10.3390/membranes13050474
43. Navarro-Tovar R., Qiu B., Martin P., Gorgojo P., and Perez-Page M., Advanced desalination performance using PVDF electrospun nanofiber membranes across multiple membrane distillation configuration, Desalination, Apr. 2025; 598, https://doi.org/10.1016/j.desal.2024.118425
44. "Infrared Spectroscopy-Analytical chemistry laboratory, ICT Prague."
45. Coates J., Interpretation of infrared spectra, a practical approach, Encyclopedia of Analytical Chemistry, Oct. 2000; 12, 101815–10837, https://doi.org/10.1002/9780470027318.a5606
46. Naseeb N., Mohammed A. A., Laoui T., and Khan Z., A novel PAN-GO-SiO_2 hybrid membrane for separating oil and water from emulsified mixture, Materials, Jan. 2019; 12(2), https://doi.org/10.3390/ma12020212
47. Rabiei M. et al., Measurement modulus of elasticity related to the atomic density of planes in unit cell of crystal lattices, Materials, Oct. 2020; 13(19), 1–17, https://doi.org/10.3390/ma13194380
48. Greiner, Andreas, and Joachim H. Wendorff, Electrospinning: A fascinating method for the preparation of ultrathin fibers, Angewandte Chemie International Edition, Jul. 2007; 46(30), 5670–5703, https://doi.org/10.1002/anie.200604646
49. Hardikar M., Felix V., Presson L. K., Rabe A. B., Ikner L. A., and Achilli A., Pore Flow and Solute Rejection in Pilot-Scale Air-Gap Membrane Distillation, 2023.
50. Kariman H., Mohammed H. A., Zargar M., and Khiadani M., Performance comparison of flat sheet and hollow fibre air gap membrane distillation: A mathematical and simulation modelling approach, J Memb Sci, Apr. 2025; 721, https://doi.org/10.1016/j.memsci.2025.123836
51. Al-Harby N. F., El Batouti M., and Elewa M. M., A comparative analysis of pervaporation and membrane distillation techniques for desalination utilising the sweeping air methodology with novel and economical pervaporation membranes, Polymers (Basel), Nov. 2023; 15(21), https://doi.org/10.3390/polym15214237
52. Gao C., Deng W., Pan F., Feng X., and Li Y., Superhydrophobic Electrospun PVDF Membranes with Silanization and Fluorosilanization Co-functionalized CNTs for Improved Direct Contact Membrane Distillation, Engineered Science, 2020, https://doi.org/10.30919/es8d905
53. Ren J., Wang X., Zhao L., Li M., and Yang W., Effective removal of dyes from aqueous solutions by a gelatin hydrogel, J Polym Environ, Nov. 2021; 29(11), 3497–3508, https://doi.org/10.1007/s10924-021-02136-z
54. Chakka A. K., Muhammed A., Sakhare P. Z., and Bhaskar N., Poultry processing waste as an alternative source for mammalian gelatin: Extraction and characterization of gelatin from chicken feet using food grade acids, Waste Biomass Valorization, Dec. 2017; 8(8), 2583–2593, https://doi.org/10.1007/s12649-016-9756-1
55. He P., Cheng H. R., Le Y., and Chen J. F., Preparation and characterization of nano-sized Sr0.7Ca0.3TiO3 crystallines by low temperature aqueous synthesis

method, Mater Lett, May 2008; 62(14), 2157–2160, https://doi.org/10.1016/j.matlet.2007.11.051

56. Geltmeyer J., Van Der Schueren L., Goethals F., De Buysser K., and De Clerck K., Optimum sol viscosity for stable electrospinning of silica nanofibres, J Solgel Sci Technol, Jul. 2013; 67(1), 188–195, https://doi.org/10.1007/s10971-013-3066-x
57. Safi N. N. et al., A systematic framework for optimizing a sweeping gas membrane distillation (SGMD), Membranes (Basel), Oct. 2020; 10(10), 1–18, https://doi.org/10.3390/membranes10100254
58. Said I. A., Chomiak T., Floyd J., and Li Q., Sweeping gas membrane distillation (SGMD) for wastewater treatment, concentration, and desalination: A comprehensive review, 2020.
59. Onsekizoglu P., Membrane distillation: Principle, advances, limitations and future prospects in food industry, in Distillation - Advances from Modeling to Applications, InTech, 2012. https://doi.org/10.5772/37625
60. Abdulhamid Alftessi S. et al., Hydrophobic silica sand ceramic hollow fiber membrane for desalination via direct contact membrane distillation, Alexandria Engineering Journal, Dec. 2022; 61(12), 9609–9621, https://doi.org/10.1016/j.aej.2022.03.044